

# 6*H*-Pyrrolo[3,2-*b*:4,5-*b'*]bis[1,4]benzothiazines: facilely synthesized semiconductors for organic field-effect transistors†

Wei Hong,<sup>a</sup> Zhongming Wei,<sup>bc</sup> Hongxia Xi,<sup>bc</sup> Wei Xu,<sup>\*b</sup> Wenping Hu,<sup>b</sup> Quanrui Wang<sup>\*a</sup> and Daoben Zhu<sup>\*b</sup>

Received 4th June 2008, Accepted 6th August 2008

First published as an Advance Article on the web 5th September 2008

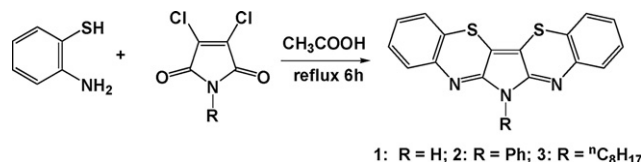
DOI: 10.1039/b809486a

6*H*-Pyrrolo[3,2-*b*:4,5-*b'*]bis[1,4]benzothiazine (PBBTZ, **1**) and its two 6-substituted derivatives (**2** and **3**) were conveniently synthesized. Their optical properties were studied by UV-vis and fluorescence spectroscopy, and electrochemical properties were investigated by cyclic voltammetry (CV). Good thermal stability was observed by thermogravimetric analysis. X-Ray analysis revealed a coplanar structure and a column stacking in the single crystal of compound **1**. OFET measurements showed that **1–3** were p-type semiconductors. The performance of these devices displayed good reproducibility at ambient conditions. When devices containing **1** were fabricated on OTS-treated SiO<sub>2</sub>/Si substrates at 60 °C, the best performance was achieved with the average hole mobility as high as 0.34 cm<sup>2</sup> V<sup>-1</sup> s<sup>-1</sup> and the on/off ratio about 10<sup>6</sup>–10<sup>7</sup>. This performance resulted from the well-ordered molecular packing as revealed by XRD and AFM analysis.

## Introduction

Over the past decade, organic field-effect transistors (OFETs) have attracted considerable interest, for their potential applications in low-cost integrated circuits and flexible electronics.<sup>1–6</sup> With regards to these advantages of OFETs, the performances of many molecules, such as mobility, on/off ratio, stability and processability, have surpassed those of amorphous hydrogenated silicon. So far, one of the best performing p-type OFET materials is pentacene, with mobility higher than 1.0 cm<sup>2</sup> V<sup>-1</sup> s<sup>-1</sup> and on/off ratio above 10<sup>6</sup>.<sup>7–9</sup> However, pentacene has several disadvantages such as oxidative instability in ambient conditions due to photo-induced decomposition to endoperoxide adducts, and extremely poor solubility in most ordinary solvents.<sup>10–13</sup> Several pentacene analogues were synthesized aimed at improving the stability, and these high-performance materials were mostly based on linear conjugated structures, such as oligoacenes,<sup>14–17</sup> oligothiophenes,<sup>5,18–20</sup> or selenophenes,<sup>21,22</sup> and N-heterocyclic oligomers.<sup>23–25</sup>

Herein, we fabricated organic thin film transistors with high performance based on facilely synthesized 6*H*-pyrrolo[3,2-*b*:4,5-*b'*]bis[1,4]benzothiazine and its 6-substituted derivatives (PBBTZ **1–3**, see Scheme 1). To the best of our awareness, this contribution represents the first investigation of these thiazine



Scheme 1 Synthesis of 6-substituted PBBTZ (**1–3**).

oligomers and their electrical properties in FET. For compound **1**, the highest mobility up to 0.34 cm<sup>2</sup> V<sup>-1</sup> s<sup>-1</sup> and the on/off ratio about 10<sup>6</sup>–10<sup>7</sup> have been obtained. These results suggest that PBBTZ systems, as good prototypes for organic semiconductors, should be promising candidates for OFETs.

PBBTZ system was first synthesized by Dimroth and Reicheneder in 1969.<sup>26</sup> In that communication, a condensation method between 2-aminothiophenol and *N*-phenyldichloromaleimide in refluxing acetic acid was concisely described, and 6-phenyl-6*H*-pyrrolo[3,2-*b*:4,5-*b'*]bis[1,4]benzothiazine (**2**) was obtained. In 1974, compound **2** was synthesized *via* another route by Kaul.<sup>27</sup> Although it has been known for almost forty years, studies on the PBBTZ system are still very limited. No more derivatives have been reported, nor have FET properties been investigated yet. Our choice of such structures was based on several reasons. Firstly, we realized that PBBTZ possessed a rigid, linear, coplanar conjugated structure similar to pentacene, yet no unit capable of a Diels–Alder reaction occurs in these molecules. Then, PBBTZ could possess a diverse library of derivatives with functionalities at the central pyrrole N atom. That may be helpful for improving the solubility, or possibly enhancing the FET performance. Furthermore, we reckoned that it could be an effective way to overcome the chemical instability of the high poly(acene)s by employing sulfur and nitrogen atoms. Taking compound **1** as an example, presumably intermolecular sulfur–sulfur interactions, and *H*-bonds between thiazine nitrogens and pyrrole hydrogens would help to form an ordered packing structure.

<sup>a</sup>Department of Chemistry, Fudan University, 200433 Shanghai, P. R. China. E-mail: qrwang@fudan.edu.cn.; Fax: +86 21 65641740; Tel: +86 21 65648139

<sup>b</sup>Beijing National Laboratory for Molecular Science, CAS Key Laboratory of Organic Solids, Institute of Chemistry, Chinese Academy of Sciences, Beijing, 100190, P. R. China. E-mail: zhudb@iccas.ac.cn; wxu@iccas.ac.cn; Fax: +86 10 62569349; Tel: +86 10 62639355

<sup>c</sup>Graduate School of Chinese Academy of Sciences, Beijing, 100039, P. R. China

† Electronic supplementary information (ESI) available: X-Ray diffraction patterns of the thin film of **2** and **3**. CCDC reference number 690390 (**1**). For ESI and crystallographic data in CIF or other electronic format see DOI: 10.1039/b809486a

## Results and discussion

### Synthesis

PBBTZ **1** and its derivatives **2–3** have been synthesized by facile one-step condensation following Dimroth's method.<sup>26</sup> Scheme 1 illustrates the synthesis route. In all cases, satisfactory yields (66–83%) were obtained. The starting material 2-aminothiophenol was readily available. More attractively, the N-functionalized 2,3-dichloromaleimides were either commercially available or easily prepared through standard reactions between 2,3-dichloromaleic anhydride and amines.<sup>28–30</sup> Our synthesis route also led to easy separation of the product. Compounds **1** and **2** were almost insoluble in the reaction system, and could be separated by simple filtration. Also, analytically pure compound **3** was obtained by column chromatography using dichloromethane as eluent. The target compounds were characterized by NMR, FT-IR, mass spectrometry (MS), and elemental analysis. The single crystal structure of **1** was determined by X-ray diffraction. The optical band gap, ionization potential, and thermal properties of PBBTZ derivatives were investigated by UV-Vis spectroscopy, cyclic voltammetry (CV) and thermal gravimetric analysis (TGA), and were compared with those of pentacene and some analogues. Finally, the field-effect performances and thin film morphologies of these compounds were examined.

### Physical properties

All the target compounds appear as orange solids and are soluble in protonic solvents, such as H<sub>2</sub>SO<sub>4</sub>–H<sub>2</sub>O and CF<sub>3</sub>CO<sub>2</sub>H. **1** is slightly soluble in THF, hot DMF and DMSO, whereas **2** and **3** are very soluble in CH<sub>2</sub>Cl<sub>2</sub>. The solids and solutions are stable in air and resist oxidation, in contrast to solutions of pentacene which are known to deteriorated in a few minutes.<sup>11,12</sup>

The normalized UV-vis absorption spectra of dilute CH<sub>2</sub>Cl<sub>2</sub> solutions and thin films of the PBBTZ samples are shown in Fig. 1(a) and (b). The main absorption peaks in solution are summarized in Table 1. The band at 240–260 nm can be assigned to the electronic transition of the phenyl ring. The fact that **1** exhibits a lower  $\lambda_{\text{max}}$  than **2** and **3** at the B-band could be explained by the decrease in  $\pi$ -conjugation which comes from intermolecular *H*-bonds. The absorption peaks at 450–490 nm, as expected, are typical of fully linear  $\pi$ -conjugation compounds. Compared with those in the solution, the absorption peaks of **1–3** in the thin film broadened and exhibited a minor red-shift of 10–30 nm, which suggested enhanced intermolecular interaction in the film states. Optical band gaps of **1–3** could be estimated from the absorption edges of the solution spectra<sup>31</sup> at about

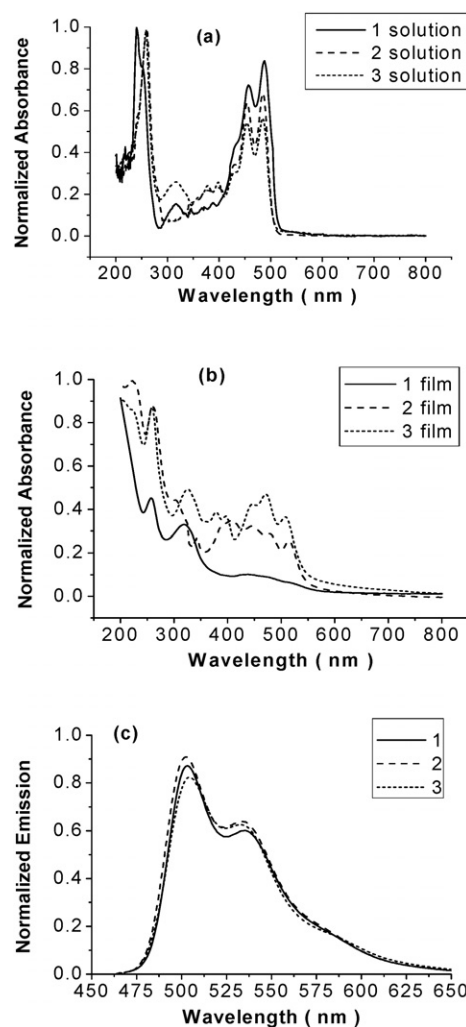


**Fig. 1** Normalized UV-vis absorption spectra of **1–3** in CH<sub>2</sub>Cl<sub>2</sub> solution (a) and thin film (b). Thin films of **2** and **3** about 50 nm thick were fabricated by vacuum-deposition methods on quartz substrates at room temperature. (c) Normalized fluorescence emission spectra of **1–3** recorded in CH<sub>2</sub>Cl<sub>2</sub> solution at room temperature.

2.41 eV, 2.44 eV, and 2.45 eV, respectively. The values obtained from the absorption edges of their thin film spectra were about 2.25 eV, larger than that of pentacene (1.77 eV), indicating higher photostability.

The dilute non-protonic solutions of **1–3** exhibit strong yellow-green fluorescence. The normalized emission spectra of them in CH<sub>2</sub>Cl<sub>2</sub> are shown in Fig. 1(c). These spectra were virtually identical, consisting of a maximum emission at 502–504 nm and

**Table 1** Physical properties of the PBBTZ derivatives **1–3**

Compound	$\lambda_{\text{max}}^{\text{abs}}/\text{nm}^a$			$T_{\text{dec}}/^\circ\text{C}$	$E_{\text{g}}^{\text{opt}}/\text{V}^a$	$E_{\text{ox}}^{\text{onset}}/\text{V}$	Energy level	
	Peak 1	Peak 2	Peak 3				HOMO/eV	LUMO/eV
<b>1</b>	240	457	488	386	2.41	1.04	−5.44	−3.03
<b>2</b>	260	454	485	324	2.44	0.95	−5.35	−2.91
<b>3</b>	258	454	485	310	2.45	0.88	−5.28	−2.83

<sup>a</sup> Solution sample in CH<sub>2</sub>Cl<sub>2</sub>.

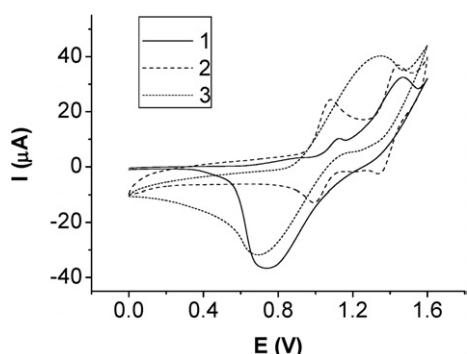


**Fig. 2** Cyclic voltammograms of **1–3** in 0.1 M (n-Bu)<sub>4</sub>NClO<sub>4</sub> in CH<sub>2</sub>Cl<sub>2</sub>, scan rate 50 mV s<sup>-1</sup>.

a shoulder at 533–535 nm, which indicated that 6-substituted groups had little influence on the excited-state energies of the PBBTZ system.

The cyclic voltammetry (CV) measurement of **1–3** was carried out in CH<sub>2</sub>Cl<sub>2</sub> using an Ag/AgCl reference electrode. As shown in Fig. 2, **1** and **2** showed two oxidation waves (reversible or half-reversible), while **3** had only one reversible oxidation wave. The first oxidation potentials of PBBTZ derivatives were 0.88–1.04 V, much higher than those of pentacene (0.28 V) and tetracene (0.52 V),<sup>32</sup> indicating the good stability of the PBBTZ radicals. The experiments were calibrated with the ferrocene/ferrocenium (Fc/Fc<sup>+</sup>) redox system, the HOMO levels of **1–3** were determined by  $E_{\text{HOMO}} = -[4.8 - E_{\text{FOC}} + E_{\text{ox}}^{\text{onset}}] \text{ eV} \approx -[4.4 + E_{\text{ox}}^{\text{onset}}] \text{ eV}$  according to the literature.<sup>31</sup> The onset oxidation potential of **1** was 1.04 V and therefore the HOMO level of **1** was estimated to be -5.44 eV. Comparably, the estimated HOMO level of **2** was about -5.35 eV, and that of **3** was about -5.28 eV. The low-lying HOMO levels accounted for the high oxidation stability of **1–3**. The HOMO levels also match well with the workfunction of metallic gold (-5.2 eV),<sup>33</sup> which could enhance the hole charge injection between the electrode and semiconductor, and thus improve the device performance. According to the HOMO level and the HOMO–LUMO gap obtained from the absorption edge in the UV-vis spectra, the LUMO levels of **1–3** were estimated to be -3.03 eV, -2.91 eV and -2.83 eV.

The thermal properties of **1–3** were investigated by thermogravimetric analysis (TGA, see Fig. 3). The thermal decomposition temperatures of **1–3** observed were about 386 °C, 324 °C and

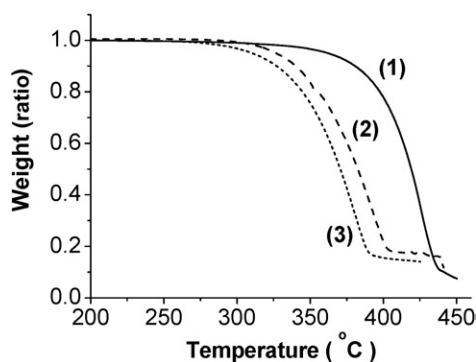


**Fig. 3** TGA plots of **1–3** with a heating rate of 10 °C min<sup>-1</sup> under N<sub>2</sub>.

310 °C, respectively, while pentacene decomposed at nearly 330 °C. These results demonstrated that the PBBTZ system is thermally stable. However, substitution at the pyrrole N atom would decrease the decomposition temperature.

### X-Ray single-crystal analysis

Orange needle-shaped single crystals of **1** were obtained by slow vacuum sublimation in a temperature-gradient furnace. X-Ray single-crystal analysis revealed the exact packing structure of the planar **1** molecule (Fig. 4a). **1** forms a monoclinic unit cell and belongs to the *P21/n* space group with the unit cell parameters  $a = 4.7896 \text{ \AA}$ ,  $b = 23.3891 \text{ \AA}$ ,  $c = 11.4926 \text{ \AA}$ ,  $\alpha = 90^\circ$ ,  $\beta = 97.347^\circ$ ,  $\gamma = 90^\circ$ . Fig. 4b and c show the stacking pattern of molecule **1** in the crystal. It can be seen that the molecules were linked to adjacent ones (symm:  $-x + 1, -y + 2, -z + 1$ ) through intermolecular hydrogen bonds (N–H⋯N, C–H⋯N) to form dimers. These dimers packed into columns along the *a*-axis direction. Intermolecular  $\pi$ – $\pi$  interactions could be observed in the column with an inter-plane distance of about 3.401 Å. These columns were linked through S⋯S non-bonding interactions to form layer structures within the *a*–*c* plane.

### X-Ray diffraction

To investigate the crystallinity and preferred orientations of the molecules **1–3**, the X-ray diffraction (XRD) of the thin films deposited on OTS/SiO<sub>2</sub>/Si (octadecyltrichlorosilane treated SiO<sub>2</sub>/Si) substrate at various temperatures ( $T_{\text{sub}}$ ) was performed. A series of sharply resolved peaks assignable to multiple (00) reflections suggest that **1** formed a highly crystalline layer structure in thin films (see Fig. 5). These diffraction peaks are different from that of the simulated powder diffraction pattern

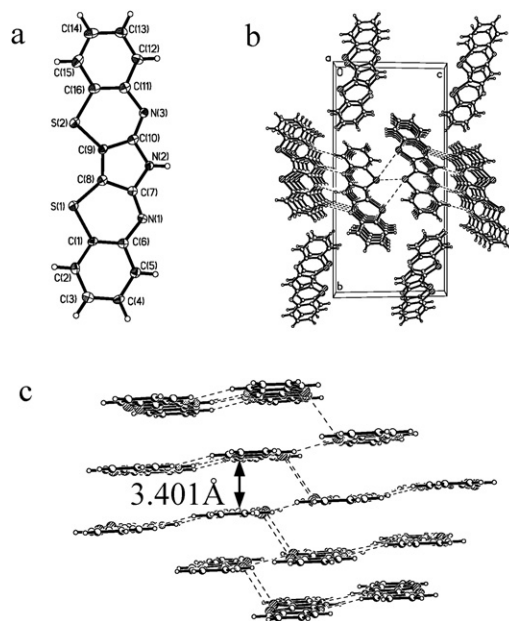


**Fig. 4** X-Ray crystal structure of compound **1**: (a) molecular structure of **1** with 50% probability ellipsoids; (b) column stacking of **1** view along the *a*-axis; (c) face to face stacking of **1** in the crystal.

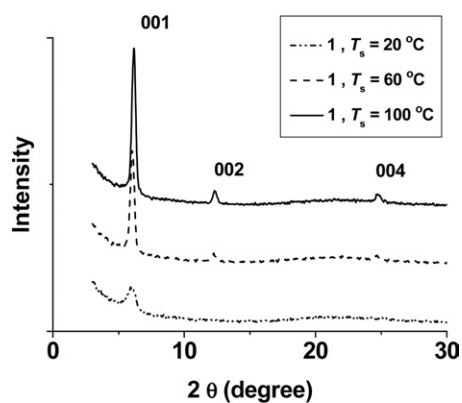


**Fig. 5** X-Ray diffraction patterns of the thin film of **1** deposited on OTS/SiO<sub>2</sub>/Si substrate at various substrate temperatures ( $T_{\text{sub}}$ ).

according to the single crystal structure of compound **1**, indicating a different stacking pattern in the thin films. The first stronger peak at 6.02° refers to a  $d$ -spacing of 1.47 nm. This value is close to that of the molecular length along its long axis (1.33 nm). Considering the intermolecular van der Waals distances, molecules of **1** must be packed almost perpendicular on the substrate. It can be observed that the intensity of the diffractions increased with increasing substrate temperature, indicating an increase of the crystallinity of the thin films. Thin films of compound **2** displayed several weak diffraction peaks, which showed a multicrystal character of these films (see ESI†). For compound **3**, diffraction peaks could only be observed for the films deposited at 60 °C as a series of (00 $l$ ) reflections. The first strong peak at 3.94° showed a  $d$ -spacing of 2.24 nm (see ESI†). This value is larger than the molecular size of compound **3**. So, the molecular stacking of **3** in the thin film could not be derived from its diffraction data.

### Film morphology

It is generally recognized that the performances of FET devices strongly depend upon their thin-film morphology. 50 nm thick films of **1–3** deposited on OTS-treated SiO<sub>2</sub>/Si substrates at various substrate temperatures were investigated by atomic force microscopy (AFM) (see Fig. 6). All the films were fabricated by the vacuum-deposition method. When the substrate temperature was at room temperature (20 °C), the film of **1** was smooth with some small grains with an average diameter of about 100 nm. When the substrate temperature was 60 °C, larger and interconnected crystal grains with a length exceeding 1 μm were observed and the film became very ordered. When the substrate temperature increased to 100 °C, the grains became much larger and varied in shape for the film. However, film discontinuity and large gaps increased as well. For the films of **2** and **3**, the trend of film morphology was similar and corresponded to their FET characteristics, too. High quality of the film may be beneficial for the elimination of the disordering effect and hence provide high mobility. As the substrate temperature was increased to 100 °C, the film of **3** became cracked and lamellar crystalline grains were observed, which led to contact problems and the vanishing of the field effect.

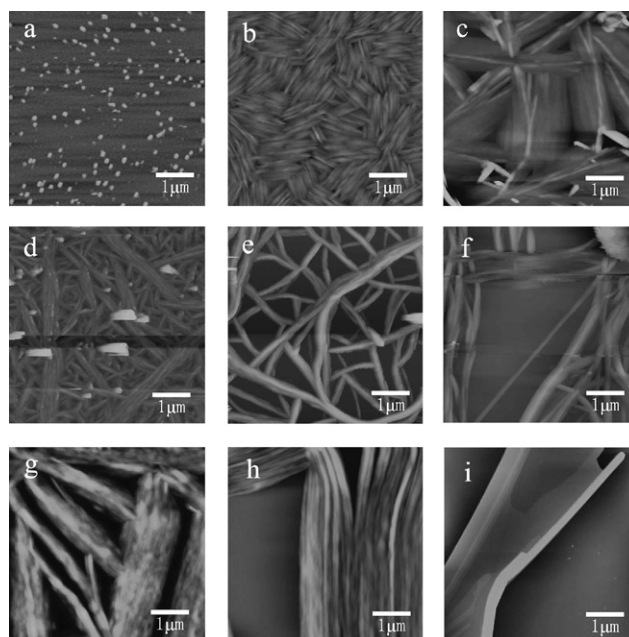


**Fig. 6** AFM images (5 × 5 μm) of 50 nm thick films of **1–3**, deposited on OTS/SiO<sub>2</sub>/Si substrates: (a) **1**,  $T_{\text{sub}} = 20$  °C; (b) **1**,  $T_{\text{sub}} = 60$  °C; (c) **1**,  $T_{\text{sub}} = 100$  °C; (d) **2**,  $T_{\text{sub}} = 20$  °C; (e) **2**,  $T_{\text{sub}} = 60$  °C; (f) **2**,  $T_{\text{sub}} = 100$  °C; (g) **3**,  $T_{\text{sub}} = 20$  °C; (h) **3**,  $T_{\text{sub}} = 60$  °C; (i) **3**,  $T_{\text{sub}} = 100$  °C.

### FET characteristics

Thin-film transistors of PBBTZ **1–3** were fabricated on OTS/SiO<sub>2</sub>/Si substrates in a top-contact configuration using Au as source and drain electrodes. The results at different temperatures are listed in Table 2. All these compounds performed as p-channel semiconductors. The mobility of devices was determined in the saturation regime using the equation  $I_{\text{DS}} = \mu C_i (V_{\text{G}} - V_{\text{T}})^2 W/2L$ , where  $I_{\text{DS}}$  is the drain–source current,  $\mu$  is the field-effect mobility,  $C_i$  is the capacitance of the gate dielectric per unit area (7.5 nF cm<sup>-2</sup>),  $W$  is the channel width,  $L$  is the channel length, and  $V_{\text{T}}$  is the threshold voltage.

It can be seen from Table 2 that FET performances largely depend on the substrate temperature. The mobility was rather low at room temperature (20 °C). Higher deposition temperatures greatly enhanced the mobility and on/off ratio, especially for compound **1**. The best performances of all devices were

**Table 2** OFET characteristics of compounds **1–3** deposited on OTS/SiO<sub>2</sub>/Si at different substrate temperatures. The mobilities were the average values of 7 typical devices

Compound	$T_{\text{sub}}/^{\circ}\text{C}$	Mobility/ cm <sup>2</sup> V <sup>-1</sup> s <sup>-1</sup>	$I_{\text{on}}/I_{\text{off}}$ ratio	Threshold voltage/V
<b>1</b>	20	$8.48 \times 10^{-4}$	$10^3$ – $10^4$	$-11.9 \pm 2.5$
	60	0.34	$10^6$ – $10^7$	$-28.0 \pm 5.7$
	100	0.068	$10^6$ – $10^7$	$-26.0 \pm 3.2$
<b>2</b>	20	$8.65 \times 10^{-5}$	$1$ – $5 \times 10^4$	$-39.8 \pm 5.0$
	60	$1.77 \times 10^{-4}$	$10^4$ – $10^5$	$-16.8 \pm 4.8$
	100	$8.17 \times 10^{-5}$	$1$ – $2 \times 10^4$	$-27.7 \pm 5.3$
<b>3</b>	20	$6.88 \times 10^{-4}$	$10^4$ – $10^5$	$-16.2 \pm 3.6$
	60	$3.01 \times 10^{-3}$	$1$ – $5 \times 10^5$	$-13.6 \pm 5.1$
	100	No field effect		

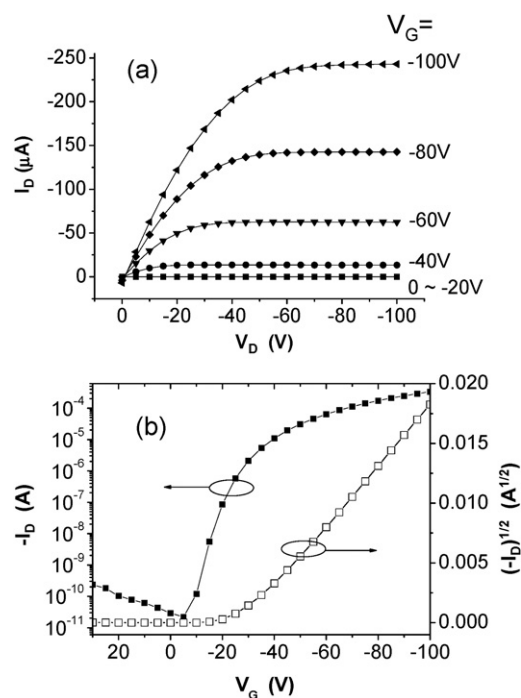


**Fig. 7** The typical output (a) and transfer (b) ( $V_D = 100$  V) characteristics of FET devices of **1** on OTS-treated  $\text{SiO}_2/\text{Si}$  substrate ( $T_{\text{sub}} = 60$  °C).

reached at 60 °C. For the FET device based on **1**, an average mobility of  $0.34 \text{ cm}^2 \text{ V}^{-1} \text{ s}^{-1}$  and an on/off ratio up to  $10^6$ – $10^7$  were achieved, which were higher than those of the devices based on **2** and **3**. Compared with compound **1**, the substituents of phenyl and alkyl groups might retard the efficient  $\pi$ – $\pi$  interactions, resulting in decreased charge transport properties. Fig. 7 shows the typical output and transfer characteristics of the device based on **1** at 60 °C. However, when the substrate temperature was further enhanced to 100 °C, the mobility of the devices of **1** and **2** decreased again. Compared with the mobility of most pentacene analogues at high temperature,<sup>1</sup> the value obtained from **1** was still promising. No field effect was found at 100 °C for the device of **3**, possibly because of the discontinuity of the thin film.

During a period of 8 weeks storage in a desiccator, the mobility of the device of **1** deposited at 60 °C changed very slightly, with the corresponding on/off ratio maintained on the order of

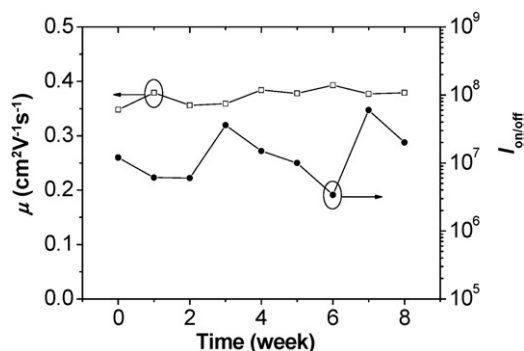


**Fig. 8** Mobility and on/off ratio for a FET device based on **1** tested over a period of eight weeks.

$10^6$ – $10^7$ , as shown in Fig. 8. All the results indicate that 6-*H* PBBTZ **1** is a high-performance stable p-type organic semiconductor.

## Experimental

### Instrumentation

<sup>1</sup>H-NMR (400 MHz) and <sup>13</sup>C-NMR (100 MHz) spectra were obtained on a Bruker DMX-400 NMR spectrometer at room temperature. EI mass spectra were collected on a GCI-MS micromass UK spectrometer. IR spectra were recorded on a Tensor 27 FT-IR spectrometer. UV-vis spectra were recorded on a Hitachi U-3010 spectrophotometer. Thermal gravimetric analysis of these molecules was conducted on a TA Instruments DTG60 TGA. A heating rate of  $10$  °C  $\text{min}^{-1}$  under flowing  $\text{N}_2$  was used with runs being conducted from room temperature to high temperature. Cyclic voltammetric measurements were recorded on a CHI660C voltammetric analyzer (CH Instruments, USA). They were carried out in a conventional three-electrode cell using Pt button working electrodes of 2 mm diameter, a platinum wire counter electrode, and a Ag/AgCl reference electrode at room temperature. Conditions: 0.1 M (n-Bu)<sub>4</sub>ClO<sub>4</sub> in dichloromethane. X-Ray diffraction measurements of thin films were performed in reflection mode at 40 kV and 200 mA with Cu K $\alpha$  radiation using a 2 kW Rigaku X-ray diffractometer. Atomic force microscopy (AFM) images of the organic thin films were obtained on a Nanoscope IIIa AFM (Digital Instruments) operating in tapping mode.

The single crystals of **1** were obtained by vacuum sublimation. X-Ray crystallographic data were collected with a Bruker Smart CCD diffractometer, using graphite-monochromated Mo K $\alpha$  radiation ( $\lambda = 0.71073$  Å). The data were collected at 113 K and the structure was resolved by the direct method and refined by full-matrix least-squares on  $F^2$ . The computation was performed with the SHELXL-97 program.<sup>34</sup> All non-hydrogen atoms were refined anisotropically.

### Material synthesis and characterization

Chemicals were purchased from Alfa Aesar, Fluka and used as received. Solvents and other common reagents were obtained from the Beijing Chemical Plant and purified as usual. N-substituted 2,3-dichloromaleimides were synthesized conveniently from 2,3-dichloromaleic anhydride according to the literature.<sup>28–30</sup>

6-*H*-Pyrrolo[3,2-*b*:4,5-*b'*]bis[1,4]benzothiazine (**1**) was produced as follows. A mixture of 2-aminothiophenol (1.002 g, 8 mmol) and 2,3-dichloromaleimide (0.664 g, 4 mmol) was dissolved in 24 mL of acetic acid. The reaction mixture was refluxed under nitrogen atmosphere for 6 h. The dark precipitate from the reaction mixture was collected. The crude product was washed several times with methanol, acetone and THF. **1** was obtained as an orange powder in a yield of 83% (1.02 g). An analytical sample was prepared by vacuum sublimation as fresh orange needles. Anal. calcd for: C<sub>16</sub>H<sub>9</sub>N<sub>3</sub>S<sub>2</sub>: C 62.52, H 2.95, N 13.67, S 20.86; found: C 62.43, H 2.97, N 13.55, S 20.97%. MS (EI<sup>+</sup>) 307. <sup>1</sup>H-NMR (CF<sub>3</sub>CO<sub>2</sub>D):  $\delta$  (ppm) 7.90–7.92 (m, 2H, Ar-H), 7.86–7.88 (m, 2H, Ar-H), 7.77–7.82 (m, 4H, Ar-H), 1.50 (s, 1H, N-H). IR (KBr disc,  $\text{cm}^{-1}$ ): 3446, 2947, 2772, 1632, 1572, 1360, 1122, 753.

Compound **2** was prepared as described above for compound **1**, from 2-aminothiophenol (1.252 g, 10 mmol) and *N*-phenyl-2,3-dichloromaleimide (1.210 g, 5 mmol). Yield: 1.42 g, 74%. An analytical sample was prepared by vacuum sublimation as fresh orange powder. Anal. calcd for: C<sub>22</sub>H<sub>13</sub>N<sub>3</sub>S<sub>2</sub>: C 68.90, H 3.42, N 10.96; found: C 68.97, H 3.49, N 10.92%. MS (EI<sup>+</sup>) 383. <sup>1</sup>H-NMR (CF<sub>3</sub>CO<sub>2</sub>D): δ (ppm) 7.88–7.92 (m, 1H), 7.81–7.85 (m, 2H), 7.69–7.73 (m, 4H), 7.54–7.62 (m, 6H). IR (KBr disc, cm<sup>-1</sup>): 3442, 3050, 1610, 1500, 1457, 1435, 1408, 1130, 949, 752, 687.

Compound **3** was prepared as described above for compound **1**, from 2-aminothiophenol (1.252 g, 10 mmol) and *N*-octyl-2,3-dichloromaleimide (1.391 g, 5 mmol). The residue was purified by column chromatography on silica gel (CH<sub>2</sub>Cl<sub>2</sub>) to afford 1.38 g (66% yield) of **3** as fine orange needles. Anal. calcd for: C<sub>24</sub>H<sub>25</sub>N<sub>3</sub>S<sub>2</sub>: C 68.70, H 6.01, N 10.01; found: C 68.28, H 5.91, N 9.98%. MS (EI<sup>+</sup>) 419. HRMS (EI<sup>+</sup>): calcd for: C<sub>24</sub>H<sub>25</sub>N<sub>3</sub>S<sub>2</sub> 419.1490, found 419.1492. <sup>1</sup>H-NMR (CDCl<sub>3</sub>): δ (ppm) 7.48–7.50 (m, 2H, Ar–H), 7.22–7.25 (m, 4H, Ar–H), 7.08–7.12 (m, 2H, Ar–H), 4.13–4.16 (t, *J* = 7.2 Hz, 2H, N–CH<sub>2</sub>), 1.80–1.84 (m, 2H, CH<sub>2</sub>), 1.35–1.39 (m, 4H, 2CH<sub>2</sub>), 1.28–1.30 (m, 6H, 3CH<sub>2</sub>), 0.85–0.89 (t, *J* = 6.6 Hz, 3H, CH<sub>3</sub>). <sup>13</sup>C-NMR (CDCl<sub>3</sub>): δ (ppm) 150.53, 140.88, 130.25, 127.48, 126.03, 125.42, 118.41, 109.62, 40.28, 32.05, 29.37, 29.35, 28.69, 26.87, 22.82, 14.25. IR (KBr disc, cm<sup>-1</sup>): 3447, 2918, 2850, 1609, 1568, 1459, 1369, 1093, 756.

*N*-Octyl-2,3-dichloromaleimide was prepared from 2,3-dichloromaleic anhydride and *n*-octylamine according to the same method for preparing the known compound *N*-octylmaleimide<sup>30</sup> and purified by flash chromatography on silica gel (EtOAc and petroleum ether, 1 : 5). Mp 44–46 °C, MS (EI<sup>+</sup>) 241, <sup>1</sup>H-NMR (CDCl<sub>3</sub>): δ (ppm) 3.57–3.60 (t, *J* = 7.1 Hz, 2H, N–CH<sub>2</sub>), 1.59–1.61 (m, 2H, CH<sub>2</sub>), 1.26–1.28 (m, 10H, 5CH<sub>2</sub>), 0.86–0.89 (t, *J* = 6.5 Hz, 3H, CH<sub>3</sub>). IR (KBr disc, cm<sup>-1</sup>): 3495, 2975, 2916, 1730, 1626, 1465, 1375, 1195, 1062, 1005, 937, 880, 732, 633.

### Device fabrication

OFET devices were fabricated in the top-contact device configuration. The substrate was a heavily doped, *n*-type Si gate electrode with a 500 nm thick SiO<sub>2</sub> layer as the gate dielectric. The gate dielectric was treated with octadecyltrichlorosilane (OTS) by the vapor deposition method. Subsequently, organic semiconductors were deposited on the substrate by thermal evaporation under a pressure of (4–6) × 10<sup>-4</sup> Pa at a deposition rate gradually increasing from 0.1 Å s<sup>-1</sup> to 0.5 Å s<sup>-1</sup> at the first 10 nm and then maintained until the thickness of the film was 50 nm. The deposition rate and film thickness were monitored by a quartz crystal microbalance (ULVAC CRTM-6000). Finally, a 20 nm thick gold source and drain electrode were deposited through a shadow mask. The channel length (*L*) and width (*W*) were 0.11 mm and 5.30 mm, respectively. The FET characteristics were measured at room temperature in air using a Keithley 4200 SCS.

### Conclusions

In conclusion, we have demonstrated a facile synthesis of three 6-substituted PBBTZ compounds **1–3**. Their physical properties

including optical, electrochemical, electrical and thermal properties were studied in detail and good thermal stability was observed. The crystal structure of **1** was investigated by X-ray single-crystal diffraction analysis and a sandwich-herringbone arrangement in the single crystal was found. FET devices based on **1–3** were successfully fabricated and they all performed as *p*-type semiconductors. The best performance was recorded when the devices based on **1** was fabricated on OTS-treated SiO<sub>2</sub>/Si substrates at 60 °C, with the average hole mobility up to 0.34 cm<sup>2</sup> V<sup>-1</sup> s<sup>-1</sup> and the on/off ratio about 10<sup>6</sup>–10<sup>7</sup>. The devices showed good stability in terms of mobility and on/off ratio for several weeks. The well-ordered molecular packing mode may account for this good performance.

### Acknowledgements

We thank the National Natural Science Foundation of China (Grants 20572113, 20632020, 20721061), State Key Basic Research Program (2006CB806201) and Chinese Academy of Sciences for financial support.

### References

- 1 A. R. Murphy and J. M. J. Fréchet, *Chem. Rev.*, 2007, **107**, 1066.
- 2 J. Zaumseil and H. Sirringhaus, *Chem. Rev.*, 2007, **107**, 1296.
- 3 Y. Sun, Y. Liu and D. Zhu, *J. Mater. Chem.*, 2005, **15**, 53.
- 4 M. L. Tang, A. D. Reichardt, N. Miyaki, R. M. Stoltenberg and Z. Bao, *J. Am. Chem. Soc.*, 2008, **130**, 6064.
- 5 T. Yamamoto and K. Takimiya, *J. Am. Chem. Soc.*, 2007, **129**, 2224.
- 6 N. J. Nishida, D. Kumaki, S. Tokito and Y. Yamashita, *J. Am. Chem. Soc.*, 2006, **128**, 9598.
- 7 H. Klauk, M. Halik, U. Zshieschang, G. Schmid, W. Radlik and W. Weber, *J. Appl. Phys.*, 2002, **92**, 5259.
- 8 C. D. Sheraw, L. Zhou, J. R. Huang, D. J. Gundlach, T. N. Jackson, M. G. Kane, I. G. Hill, M. S. Hammond, J. Campi, B. K. Greening, J. Francl and J. West, *Appl. Phys. Lett.*, 2002, **80**, 1088.
- 9 D. J. Gundlach, Y. Y. Lin, T. N. Jackson, S. F. Nelson and D. G. Schlom, *IEEE Electron Device Lett.*, 1997, **18**, 87.
- 10 M. Yamada, I. Ikemoto and H. Kuroda, *Bull. Chem. Soc. Jpn.*, 1988, **61**, 1057.
- 11 A. Maliakal, K. Raghavachari, H. Katz, E. Chandross and T. Siegrist, *Chem. Mater.*, 2004, **16**, 4980.
- 12 P. Coppo and S. G. Yeates, *Adv. Mater.*, 2005, **17**, 3001.
- 13 H. Meng, M. Bendikov, G. Mitchell, R. Helgeson, F. Wudl, Z. Bao, T. Siegrist, C. Kloc and C. H. Chen, *Adv. Mater.*, 2003, **15**, 1090.
- 14 J. E. Anthony, *Chem. Rev.*, 2006, **106**, 5028.
- 15 C. D. Sheraw, T. N. Jackson, D. L. Eaton and J. E. Anthony, *Adv. Mater.*, 2003, **15**, 2009.
- 16 H. Moon, R. Zeis, E.-J. Borkent, C. Besnard, A. J. Lovinger, T. Siegrist, C. Kloc and Z. Bao, *J. Am. Chem. Soc.*, 2004, **126**, 15322.
- 17 A. L. Briseno, Q. Miao, M.-M. Ling, C. Reese, H. Meng, Z. Bao and F. Wudl, *J. Am. Chem. Soc.*, 2006, **128**, 15576.
- 18 *Handbook of Oligo- and Polythiophenes*, ed. D. Fichou, Wiley-VCH, Weinheim, 1999.
- 19 D. Fichou, *J. Mater. Chem.*, 2000, **10**, 571.
- 20 J. Chisaka, M. Lu, S. Nagamatsu, M. Chikamatsu, Y. Yoshida, M. Goto, R. Azumi, M. Yamashita and K. Yase, *Chem. Mater.*, 2007, **19**, 2694.
- 21 Y. Kunugi, K. Takimiya, K. Yamane, K. Yamashita, Y. Aso and T. Otsubo, *Chem. Mater.*, 2003, **15**, 6.
- 22 K. Takimiya, Y. Kunugi, Y. Konda, N. Niihara and T. Otsubo, *J. Am. Chem. Soc.*, 2004, **126**, 5084.
- 23 S. Cherian, C. Donley, D. Mathine, L. LaRussa, W. Xia and N. J. Armstrong, *J. Appl. Phys.*, 2004, **96**, 5638.
- 24 Y. Wu, Y. Li, S. Gardner and B. S. Ong, *J. Am. Chem. Soc.*, 2005, **127**, 614.
- 25 Y. Li, Y. Wu, S. Gardner and B. S. Ong, *Adv. Mater.*, 2005, **17**, 849.

- 
- 26 P. Dimroth and F. Reicheneder, *Angew. Chem., Int. Ed. Engl.*, 1969, **8**, 751.
- 27 B. L. Kaul, *Helv. Chim. Acta*, 1974, **57**, 2664.
- 28 Y. L. Chow and Y. M. A. Naguib, *J. Chem. Soc., Perkin Trans. 1*, 1984, **6**, 1165.
- 29 Y. Mao, I. Maley and W. H. Watson, *J. Chem. Crystallogr.*, 2005, **35**, 385.
- 30 A. S. Kalgutkar, B. C. Crews and L. J. Marnett, *J. Med. Chem.*, 1996, **39**, 1692.
- 31 X. Gao, W. Wu, Y. Liu, S. Jiao, W. Qiu, G. Yu, L. Wang and D. Zhu, *J. Mater. Chem.*, 2007, **17**, 736.
- 32 R. Schmidt, S. Göttling, D. Leusser, D. Stalke, A. M. Krause and F. Würthner, *J. Mater. Chem.*, 2006, **16**, 3708.
- 33 N. Drolet, J. F. Morin, N. Leclerc, S. Warkim, Y. Tao and M. Leclerc, *Adv. Funct. Mater.*, 2005, **15**, 1671.
- 34 G. M. Sheldrick, *SHELXL-97, Program for refinement of crystal structures*, University of Göttingen, Germany, 1997.